

# TENSILE STRENGTH OF PAPER REVISITED

*Kaarlo Niskanen, Jari Sirviö and Rolf Wathén*

KCL Science and Consulting, P.O.Box 70, FIN-02151 ESPOO, FINLAND

## ABSTRACT

Traditional micromechanical theories for the tensile strength of paper do not account for the tensile stiffness of paper, even though in practice tensile strength is closely coupled with tensile stiffness. Another problem is with the micromechanical input parameters, few of which have a precise meaning in real paper. Especially the interpretation of inter-fiber bonding is ambiguous. None of the existing theories connects tensile strength with an *independently* measurable value of bonding degree or bond strength. As a result, the conventional interpretation of tensile strength data is unreliable.

In this paper we will present a “macromechanical” study that connects tensile strength with independently measured values of tensile stiffness and z-directional fracture energy (alternatively Scott bond or z-directional tensile index). The model expression agrees well with many – but not all – of the experimental datasets that we had available. The disagreements demonstrate that z-directional measurements do not capture some aspects of inter-fiber bonding that contribute to in-plane tensile strength.

## 1 INTRODUCTION

For decades, various micromechanical models have been published for the tensile strength of paper [1]–[8]. The differences and similarities between

them have been actively discussed in the literature, to our knowledge the most recent and comprehensive study being in Ref. [9]. These models are often used because they provide a simple coupling, in the form of explicit equations, between the tensile strength of paper and some apparently well-defined properties of fibers and sheet structures. Such a theoretical framework would naturally be useful in the development of better paper. Unfortunately, we believe that the above-mentioned models for tensile strength are unreliable. They do not give the right information about the role of fiber properties or sheet structures. For example, consider the following two problems.

First, micromechanical models always consider the strength of a typical or representative microscopic fiber assembly. But does failure occur at a typical average location? Probably it does not. Yet numerous experiments demonstrate that changes in tensile stiffness control changes in tensile strength, see for example the analysis of Seth and Page [10]. Tensile stiffness in turn is definitely an average property of the entire fiber network. Our experience is that in machine-made papers, the ratio of tensile index over tensile stiffness is often equal  $1.0 \pm 0.1\%$ . Even in handsheets the ratio is almost exclusively between 0.5% and 1.5% [11]. Thus one would think that any micromechanical model of tensile strength would also account for tensile stiffness. This is not the case.

Second, the input parameters of micromechanical models cannot be directly measured. Many of these parameters depend on some simplification of the network structure or micromechanical stress state. Inter-fiber bonding is a good example. There exists no direct measurement for inter-fiber bond strength. It would be very tedious to measure the largely varying values that inter-fiber bond strength must have in real paper. Besides, what should be the loading mode of bonds in such an fictitious measurement? Considering the variability of local network structure, a whole range of different loading modes should be applied. Even the z-directional loading mode might have some relevance.

Even if one cannot directly measure inter-fiber bonding (whatever the precise definition), it is very clear that inter-fiber bonding is very important for tensile strength. A common but unreliable method is to compare light scattering data with tensile strength data to determine a “relative bonding area”. The result relies completely on the assumption that tensile strength is inversely proportional to light scattering. In other words, one uses tensile strength data to explain tensile strength data – a typical circular reference! The only sensible conclusion one can draw is that if light scattering decreases, inter-fiber bonding area may increase. Not even this one can be sure of. Quite certainly one *cannot* determine *values* of “relative bonded area” from light scattering data.

In this paper we will follow a different, macroscopic approach to the analysis of tensile strength. We will provide a representation based on linear elastic fracture mechanics that connects quantitatively tensile strength to macroscopic measurements of inter-fiber bonding and tensile stiffness of paper. The role of fiber strength will be added in the next phase.

On a philosophical level, the following study is one step in the application of effective medium approach to paper. Our meaning is best illustrated with an example. The classical concept of electrons as particles is useful in semiconductors, provided that one considers electrons in a generalized sense. For example, the “effective” mass of electrons depends on the medium in which they move. That effective mass can be seen in macroscopic measurements [12].

In analogy to the effective electrons in a semiconductor, it is useful to consider fibers in a paper sheet as “metafibers” whose properties are dependent on the network that the fibers have been dried into. The tensile stiffness of the “metafibers” is a good example of this [13]. Similar measures are needed for the effective inter-fiber bonding and effective fiber strength.

## **2 MACROSCOPIC APPROACH TO TENSILE STRENGTH**

### **2.1 Linear elasticity at fracture**

Our starting point is the well-known observation that the elongation of paper causes generally little change in tensile stiffness at sub-fracture strain levels (Figure 1). After elongation-recovery cycles, the stress-strain curve of paper exhibits more and more linear elasticity. If we elongate a paper sample almost to failure and then release, the resulting sample is almost perfectly linearly elastic all the way to failure. The fact that the tensile stiffness does not change indicates that there is no significant fatigue damage [14]. Tensile strength is almost independent of elongation-recovery cycles (Figure 1).

Hence, even if paper generally exhibits plastic elongation behavior, it can be considered as a linearly elastic material for the fracture properties. Donner made use of this and demonstrated [16] that linear elastic fracture mechanics does describe the tensile strength of paper, provided that one can properly measure the required macroscopic parameters. The most problematic in this sense is the critical defect size  $a$ , for which Donner had no independent measurement available. In his newsprint samples,  $a$  was close to 1 mm, *i.e.* similar to mean fiber length.

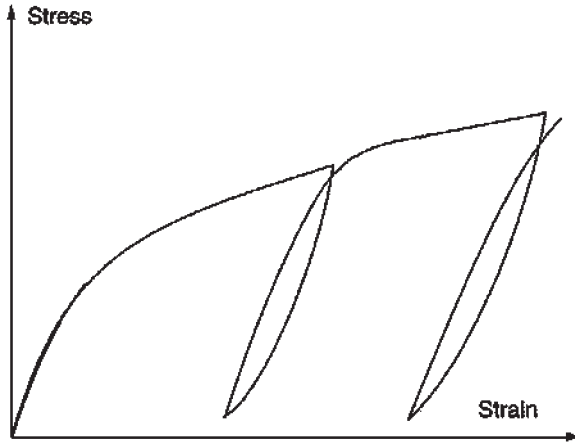


Figure 1 Stress-strain cycles in arbitrary units redrawn after [15].

## 2.2 Homogeneity

Compared to typical linearly elastic materials, the tensile strength of paper shows surprisingly little variability. If one considers the Weibull-modulus as a measure of uniformity, typical values for paper start from around 15 [17]–[19], where as typical values for glass would be 5–10 [20].

The homogeneity of tensile strength values suggests that the tensile strength of paper is not controlled by discontinuous macroscopic defects, such as holes, dirt specs, shives etc. Of course such defects do exist in paper and cause web breaks. Their effect can be seen when strength distributions are measured from large enough samples [19]. However, these defects are too rare to account for the tensile strength values that one measures in laboratory. If the opposite were true, one should be able to observe a macroscopic defect along the fracture line of every tensile specimen.

We conclude that the ordinary mean tensile strength of paper is not governed by macroscopic defects that are present in the paper from the beginning. Instead the tensile strength must, in some way, be governed by the *mean* microscopic structure and the *mean* properties of fibers. In the analysis of Donner, tensile stiffness and fracture energy are, by construction, average properties of paper. The same must apply to the critical defect size  $a$ . We should be able to understand  $a$  in the same way that we understand tensile stiffness and fracture energy.

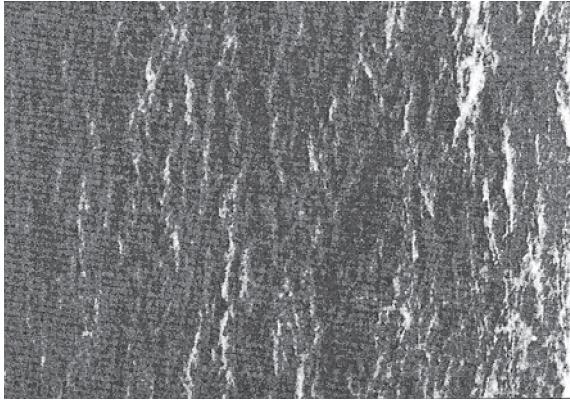


**Figure 2** Localized damage areas (shown as white) in a newsprint sample that was strained in the horizontal direction [21].

### **2.3 Damage localization**

Plastic elongation creates inhomogeneous local damage to paper (Figure 2) [21]. Some areas elongate more than others. Damage occurs when inter-fiber bonds open gradually. There is more damage in areas of high elongation than in areas of low elongation. Eventually one of the areas of high local elongation or high damage triggers the failure of the paper sample.

We find it plausible that the damage regions created during plastic elongation act qualitatively in the same way as discontinuous defects in paper. In other words, the damage area that triggers macroscopic failure corresponds to the critical defect size  $a$  estimated by Donner [16]. The sizes of damage regions in a plastically elongated paper have not yet, to our knowledge, been studied in detail. However, in terms of orders of magnitude, their sizes are similar to fiber length just as  $a$  is.

Instead of the local damage areas created in tensile testing, what we measured is the size of the fracture process zone (FPZ) when a crack starts to propagate from a cut made to the specimen (Figure 3). Fracture process zone is the area where plastic deformation and damage is distributed during the fracture. The longitudinal width of the FPZ measured after crack propagation is called damage width.

It is then tempting to assume that the damage width (measured *after* the crack has propagated from a cut) would be related to the critical defect size  $a$  that in Donner's analysis is needed to explain the tensile strength of paper. We have already shown [16] that if  $a$  is assumed equal to damage width,

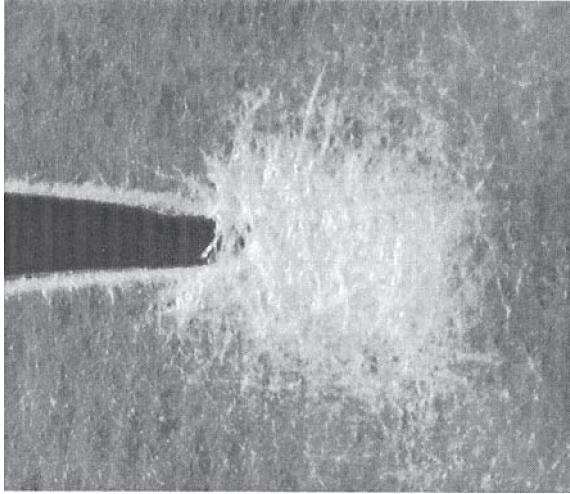


**Figure 3** Fracture process zone (FPZ, the white area) in a handsheet of pure softwood kraft. The crack is just about to start propagating to the right. The FPZ diameter is 3–4 mm [22].

reasonable agreement with measured tensile strength values can be obtained. However, the agreement we have reported does not prove that damage width is equal to  $a$ . Figure 4 shows one counter-example.

It is quite possible that one should measure the size of the local damage areas at the onset failure in the ordinary tensile test, in order to obtain a reliable measure for the critical defect size  $a$ . It is also possible that the measurements we have used are unreliable. However, for the time being, damage width is the best available *independent* estimate of  $a$ .

## 2.4 Invariance of fracture energy

Fracture energy is the energy that is consumed when fracture surface forms. When paper fails through the breakage of inter-fiber bonds, the apparent fracture surface is the area of broken inter-fiber bonds. It is also possible, even probable, that microscopic fracture surfaces open up inside fiber walls. *If* one can assume that the latter consume little energy, then fracture energy is invariantly proportional to the total area of broken inter-fiber bonds. This means that the energy consumed in breaking those bonds should be *independent of the loading mode* in which those bonds were broken.

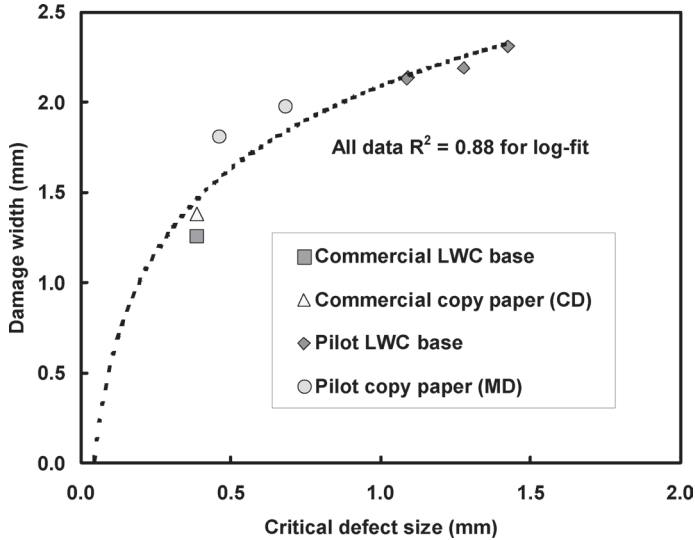


**Figure 4** Damage width against the critical defect size  $a$  determined from tensile strength [23].

Although it is highly probable that the invariance of fracture energy does not always hold, it is not bad as the first approximation. We have demonstrated [24] that in-plane fracture energy divided by damage width is, at least in some cases, closely related to different measures of out-of-plane fracture energy and out-of-plane tensile energy absorption (*i.e.* Scott bond). The invariance of fracture energy suggests that one should be able to use out-of-plane measurements of fracture energy as a measure of inter-fiber bonding in the analysis of tensile strength.

Next we will show that, indeed, the tensile index of paper can be connected to tensile stiffness, on the one hand, and either z-directional fracture energy, Scott bond or z-directional tensile index, on the other hand.

### 3 MACROSCOPIC MODEL

We will use the linear elastic fracture mechanics despite the entailed simplifications. As we have shown before [22], the tensile strength of paper is approximately given by

$$T = \frac{1}{\beta} \sqrt{\frac{GE}{2\pi w_d}} \quad (1)$$

where  $T$  is tensile index  
 $G$  is fracture energy index,  
 $E$  is tensile stiffness index  
 $w_d$  is damage width [22] and  
 $\beta$  is a geometry factor of defect and sample dimensions.

Equation (1) is the basic equation in linear elastic fracture mechanics (LEFM), excluding the factor 2, stating the relationship between strength, tensile stiffness and fracture energy. Since we want a simple expression to start with, we will assume in the following that the geometry factor can be set equal to  $\beta = 1$ . Strictly speaking  $\beta$  depends on sample geometry and the number, size and shape of the defects in that sample. Value 1 holds only when a thin plate sample has one cut like defect oriented perpendicular to the direction of loading far from the sample edges. This will cause a necessary quantitative deviation between model and measured values.

There are limitations to Equation (1) if one would like to use it to analyze tensile strength. First, fracture energy and damage width are rather tedious to measure. Measurement method influences their values to a much larger extent than it influences tensile stiffness. In addition, the three quantities, tensile stiffness, fracture energy and damage width are usually correlated in a manner suggesting they are in some way intrinsically connected. Damage width is linearly related to fiber length (unless fiber strength is low, see [25]), so Eq. (1) would seem to imply that fiber length should have a strong effect on tensile strength. In fact, fracture energy often depends linearly on damage width, thus countering for the apparent effect of fiber length in Equation (1).

These considerations lead us to try what happens if we apply the invariance of fracture energy (see Ch. 2.4) and replace  $G/w_d$  with the z-directional fracture energy  $G_z$  that is easier to measure and more precise than in-plane fracture energy and damage width separately. In order to get the dimensions right, we observe that the in-plane  $G$  measures energy consumption per unit crack length, divided by grammage. The z-directional fracture energy  $G_z$  equals energy per unit area of sheet. It corresponds to the delamination of *one* bonding interface between fiber layers. The number of such interfaces is  $b_{\text{sheet}}/b_{\text{fiber}} - 1$ , or roughly  $b_{\text{sheet}}/b_{\text{fiber}}$ . This leads to

$$\frac{G}{w_d} = \frac{G_z}{b} \cdot \frac{b}{b_{\text{fiber}}} = \frac{G_z}{b_{\text{fiber}}} \quad (2)$$



where  $b$  is sheet grammage and  $b_{fiber}$  is fiber grammage.

Equation (2) is qualitatively supported by experimental evidence [24].

What remains to be done is to determine  $G_z$ . Direct measurements of  $G_z$  include Z-toughness [26], [27] and nip-peeling energy [24]. The numbers obtained from them can be directly used in Equation (1). We recognize that neither of these tests is ideal. In Z-toughness [26] measurement the fracture process zone appears to be rather thick because of the zero peeling angle. The situation is analogous to small tearing angle in an in-plane tear test [28]. In the nip-peeling test, some energy is spent in bending [29].

When nip peeling test or z-toughness test are available, we obtain the following expression for the ordinary in-plane tensile strength of paper by combining Equation (1) and Equation (2):

$$T = \sqrt{\frac{E \cdot G_z}{2\pi \cdot b_{fiber}}}. \quad (3)$$

This expression is very appealing because the fiber grammage  $b_{fiber}$  is the only microscopic parameter. Fiber grammage is coarseness divided by fiber width  $w_{fiber}$ , and the latter can be measured from microscopic sheet images.

Indirect estimates for  $G_z$  can be obtained from Scott bond ( $W_z$ ) and z-tensile strength ( $T_z$ ), see Appendix I. For these calculations we have to make more assumptions:

1. paper is linearly elastic when loaded to fracture in z-direction (which it is not!),
2. sheet structure is homogeneous in z-direction (which it is not!), and
3. the z-directional elastic modulus of paper is proportional to sheet density, which would hold e.g. if paper were equivalent to a homogeneous medium diluted with small pores.

The assumptions lead to the following alternative expressions for the tensile strength of paper:

$$T = \sqrt{\frac{2 \cdot E \cdot W_z \cdot w_{fiber}}{\pi^2 \cdot t_{sheet} \cdot t_{fiber}} \cdot \left( \frac{1}{\rho_{sheet}} - \frac{1}{\rho_{fiber}} \right)} \quad (4)$$

when Scott bond values  $W_z$  are available (cf. Equation (A6) in Appendix), and

$$T = \sqrt{\frac{E}{\pi^2 \cdot E_{fiber} \cdot \rho_{sheet}} \cdot \frac{w_{fiber}}{t_{fiber}} \cdot \left(\frac{\rho_{fiber}}{\rho_{sheet}} - 1\right)} \cdot T_z \quad (5)$$

when z-directional tensile strength  $T_z$  is available (cf. Equation (A4) in Appendix). The other parameters in these equations are:

- $w_{fiber}$  is fiber width,
- $t_{fiber}$  is fiber thickness,
- $\rho_{sheet}$  is sheet density,
- $\rho_{fiber}$  is fiber density (= 1500 kg/m<sup>3</sup>), and
- $E_{fiber}$  is the z-directional tensile stiffness of fibers.

The physics of Expressions (4) and (5) is as follows. The density factor in parenthesis estimates the typical size of the planar pores that trigger delamination. The same density dependence has been derived for z-dimensional pores [30]. We believe that the density dependence of the mean pore size is universal. The ratio of fiber thickness and width,  $w_{fiber} / t_{fiber}$ , accounts for the anisotropy of pore structure between in-plane and out-of-plane directions.

A few comments are in order before we proceed to compare the model equations with experiments. Equations (3), (4) and (5) form a sequence of increasing complexity and increasing uncertainty. In terms of complexity, fiber grammage is the only microscopic parameter in Equation (3). In Equation (5) there are three microscopic fiber parameters. All the fiber parameters should be measured from the dry paper because the papermaking process influences them. On the other hand, in all the equations, the microscopic parameters form only a multiplying factor in front of the predicted tensile index. The effects of the individual microscopic parameters cannot be separated.

Equations (3), (4) and (5) also contain other uncertain scale factors that affect the quantitative predictions. In Equation (2), we have implicitly assumed that damage width gives the *mean* width of the zone where inter-fiber bonds break. It is probable that this assumption is inaccurate, since damage width measures the intensity of apparent bond openings down to 10%, not 50% [25]. Another source of uncertainty is the extra factor 2 in the denominator of Equation (1).

All these aspects considered, Equations (3), (4), and (5) predict tensile index up to a common but unknown geometric scale factor.

## 4 COMPARISON WITH EXPERIMENTS

We start the comparison from the z-directional fracture energy calculation, then check the influence of papermaking conditions, and finally consider different furnishes.

### 4.1 Estimation of z-directional fracture energy

In Appendix 1 we derived relationships between that can be used to estimate z-directional fracture energy  $G_z$  from either Scott Bond  $W_z$  or z-directional tensile index  $T_z$ . The first calculation is demonstrated in Figure 5. Nip-peeling test [24] was used for the z-directional fracture energy. The agreement is very good. However, in order to achieve it we had to adjust fiber width to  $w_f = 3.8\mu\text{m}$ . This is an order of magnitude less than realistic values.

The calculation of z-directional tensile strength is shown in Figure 6. The model would predict higher strength but the measurement value saturates. The saturation of high strength values presumably reflects the partial failure of the two-sided adhesive tape used in the measurements. Fiber width was

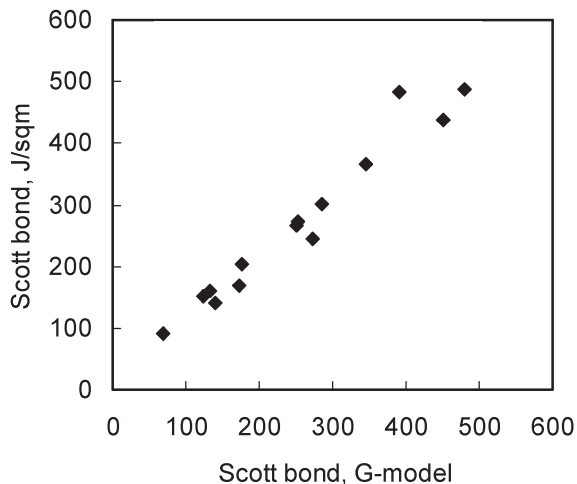


**Figure 5** Comparison of measured Scott bond values with those calculated from z-directional fracture energy (see Equation (A5)), with  $w_f = 3.8\mu\text{m}$ . Softwood kraft pulps of different refining levels (0, 1000 and 3000 revs at PFI-mill) and nip-peeling test [24] to measure  $G_z$  were used.

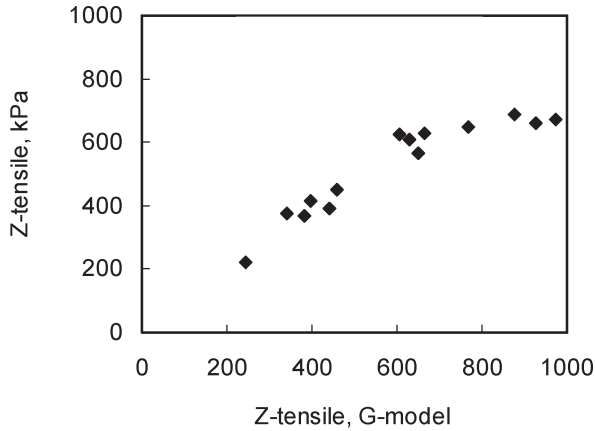


**Figure 6** Measured against calculated z-directional tensile strength, Equation (A3). The input parameters of the model were  $E_{fiber} = 150$  kPa,  $w_{fiber} = 3.8$   $\mu\text{m}$ . Same pulps as in Figure 5. Nip peeling test was used to measure  $G_z$ .

again set to  $w_f = 3.8\mu\text{m}$  and the z-directional tensile modulus of fibers was adjusted to  $E_{fiber} = 150$  kPa in order to obtain quantitative agreement below the saturation.

The tensile strength predictions for the samples in Figures 5 and 6 are shown in Figure 7. When nip peeling energy was used in Equation (3), the best agreement with experiments was obtained for the fiber grammage  $b_{fiber} = 7$   $\text{g/m}^2$ . This is quite a realistic value. With Scott bond in Equation (4), the fiber width-to-thickness ratio  $w_{fiber} / t_{fiber} = 2.0$  was best. For the calculation with z-directional tensile strength, Equation (5), we used the same modulus value  $E_{fiber} = 150$  kPa as before. In the last calculation the saturation of z-directional tensile strength values makes it impossible to reach good agreement with measured tensile index values.

To summarize the above observations, z-directional fracture energy in Equation (3) gives very good tensile strength predictions with a completely realistic value of fiber grammage. The Scott bond calculation, Equation (4), is also reasonable if one accepts the low value of fiber width. The z-directional tensile strength is not as useful in the analysis of tensile strength because of its saturation at high bonding levels.

It is rather obvious why the fiber width value has to be adjusted to an unrealistically low level in Equation (4). Of the three assumptions required in the model derivation, the first two (*i.e.* linearity and homogeneity in

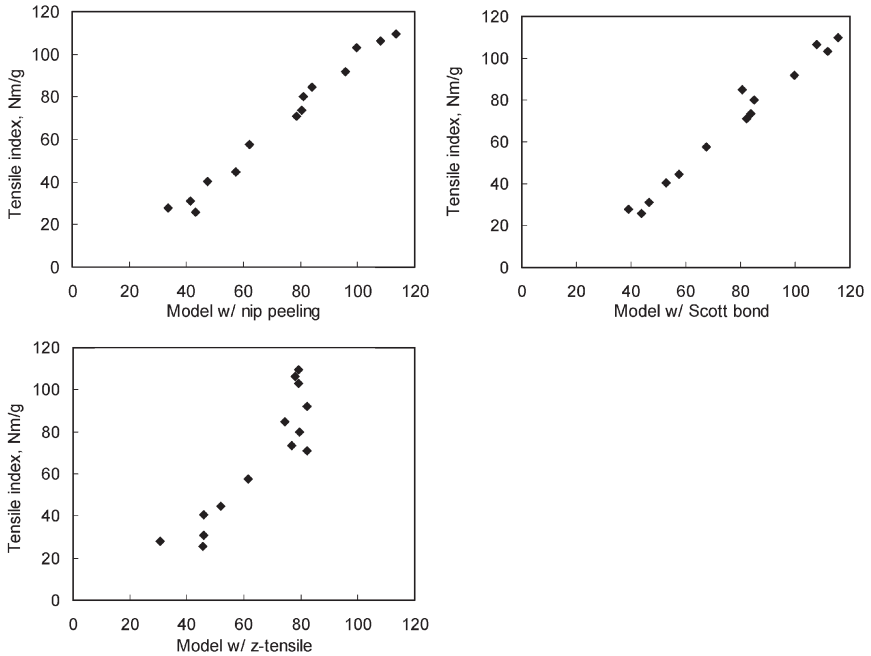


**Figure 7** Comparison of Equations (3)–(5) with experimental data for the same samples as in Figure 5. The input parameters of the three models were adjusted to  $b_{fiber} = 7 \text{ g/m}^2$ ,  $w_{fiber} / \tau_{fiber} = 2.0$ , and  $E_{fiber} = 150 \text{ kPa}$ , respectively.

z-direction) lead to an overestimate of the z-directional fracture energy. The quantitative relationship between  $W_z$  and  $G_z$  might be improved if linearity assumption is abandoned and more exact stress-strain behavior used instead. Now the error is then compensated by the small value for fiber width. It is also possible that the estimate of critical defect size  $a_z$  (Equation (A1)) is too large because of fiber twisting [31].

## 4.2 Changes in papermaking conditions

Changes in the papermaking conditions offer a good test for the validity of our macroscopic model approach. When papermaking conditions are changed, fiber dimensions in the paper remain (almost) constant. All the changes in tensile index should therefore be controlled by changes in the effective medium properties, tensile stiffness  $E$ , fracture energy  $G_z$  and density  $\rho_{sheet}$  of paper.

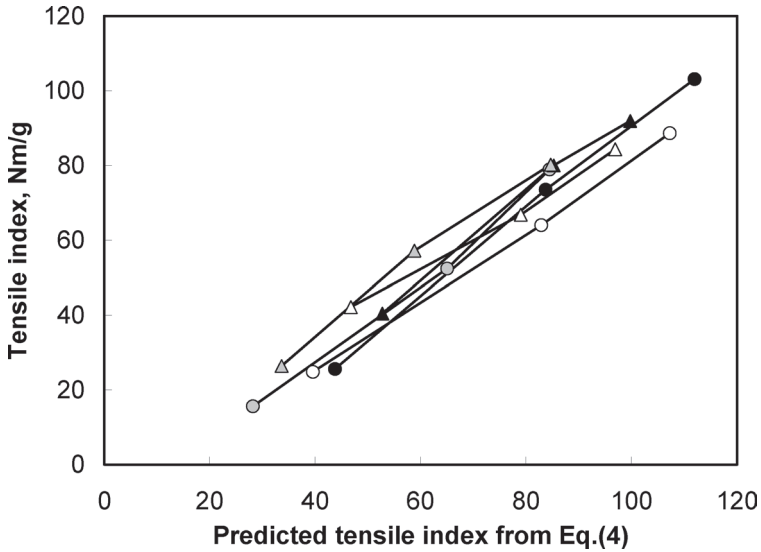


**Figure 8** Comparison of Equation (4) with experimental data on two softwood pulps. The lines connect points of a refining series (0, 1000 and 3000 revs at PFI-mill). The handsheets were either plate dried (black symbols), freely dried (white symbols) or dried under a 1% strain (gray symbols).  $w_{fiber} / t_{fiber} = 2.0$  in Equation (4).

As we saw above, z-directional fracture energy (nip peeling energy) would be the best alternative to characterize inter-fiber bonding. Unfortunately we have very little such data other than those presented above. We must thus rely on the Scott bond measurements and Equation (4). We use the ratio  $w_{fiber} / t_{fiber} = 2.0$  for consistency.

Most of the machine-made papers are strained during drying of the web, while drying shrinkage in standard handsheets is only partly prevented. Figures 8 and 9 show experimental data for handsheets that were either dried under different conditions or strained in the wet state. Equation (4) reproduces the resulting changes in tensile index. In Figure 8, the bleached kraft pulp has proportionately higher values for the measured tensile index than the unbleached kraft pulp.

Figure 10 demonstrates that Equation (4) reproduces also the influence of fiber orientation. We used the dynamic Formette sheet former to prepare the oriented handsheets from a bleached spruce pulp. The three highest measured strength values correspond to MD direction and the three lowest to CD direction.

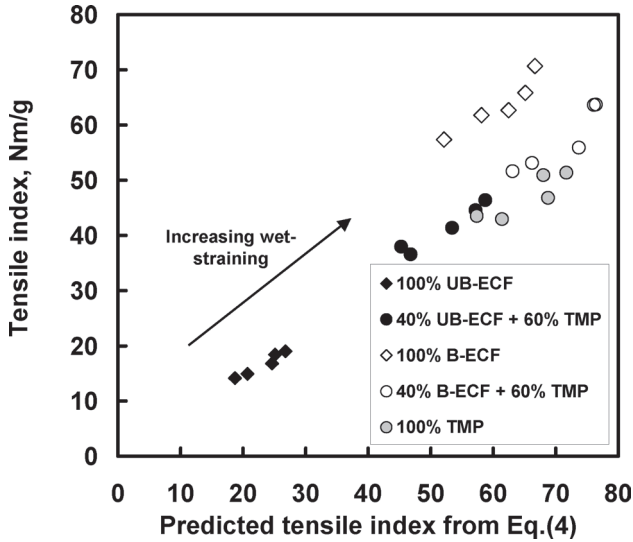


**Figure 9** Equation (4) applied to data from [32] where wet straining was altered before handsheet drying for unbleached kraft (black symbols), bleached kraft (white symbols), TMP (gray symbols) and their mixtures.  $w_{fiber} / t_{fiber} = 2.0$  in Equation (4).

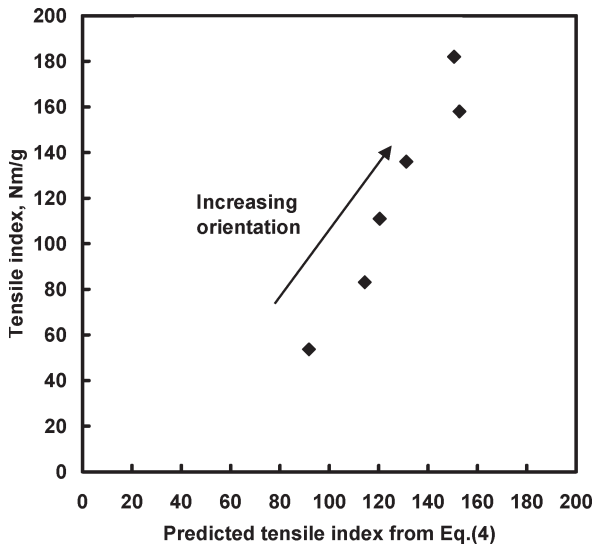


**Figure 10** Equation (4) applied to oriented handsheets made from a bleached spruce pulp with a dynamic Formette sheet former.  $w_{fiber} / t_{fiber} = 2.0$  in Equation (4).

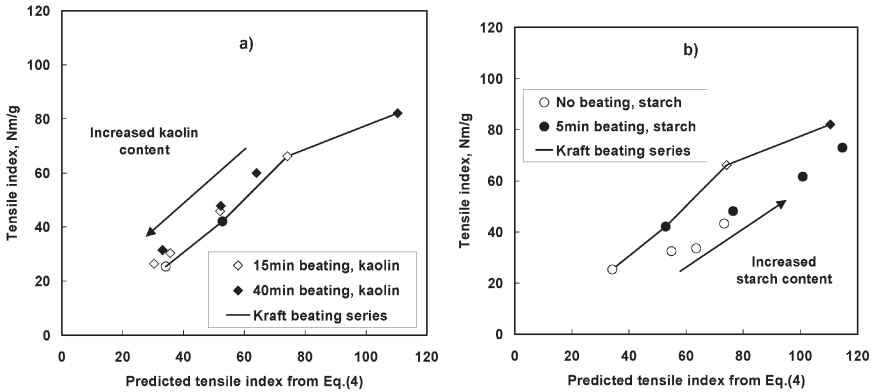


**Figure 11** Equation (4) vs. measurements for unrefined and refined softwood kraft pulps with the addition of 10 to 30% kaolin (a), and 1 to 4% starch (b). The lines connect the points of different refining levels, while the arrows indicate the direction of increasing kaolin or starch addition.  $w_{fiber} / t_{fiber} = 2.0$  in Equation (4).

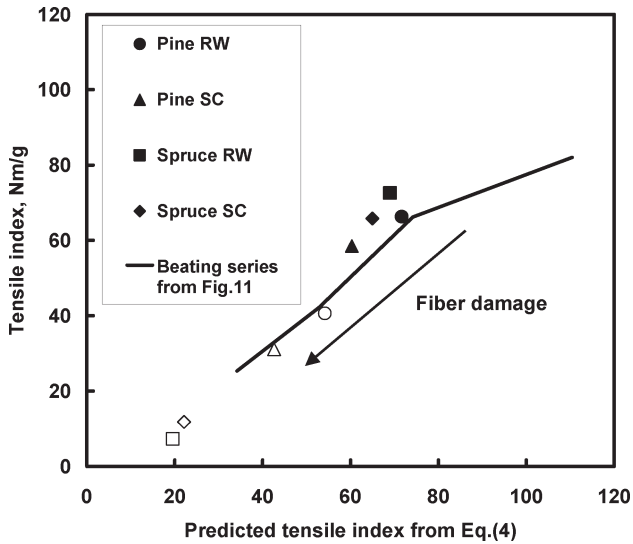
### 4.3 Furnish effects

A rather pure change in inter-fiber bonding can be achieved by adding starch or filler to the furnish, see Figure 11. When filler is present, its contribution to mass and volume (thickness and density) of the sheets must be removed from the calculations in Equation (4). Assuming that fillers do not contribute to sheet thickness, we calculated the equivalent density of the fiber network by dividing the grammage of the fiber network (=sheet grammage – filler grammage) with sheet thickness. The in-plane tensile strength and tensile stiffness were correspondingly indexed using the grammage of the fiber network. With this transformation the effect of kaolin addition is well reproduced by Equation (4). Starch addition behaves in a different manner. The first starch additions gives a sharp increase in the predicted tensile index whereas only a little change is actually observed.

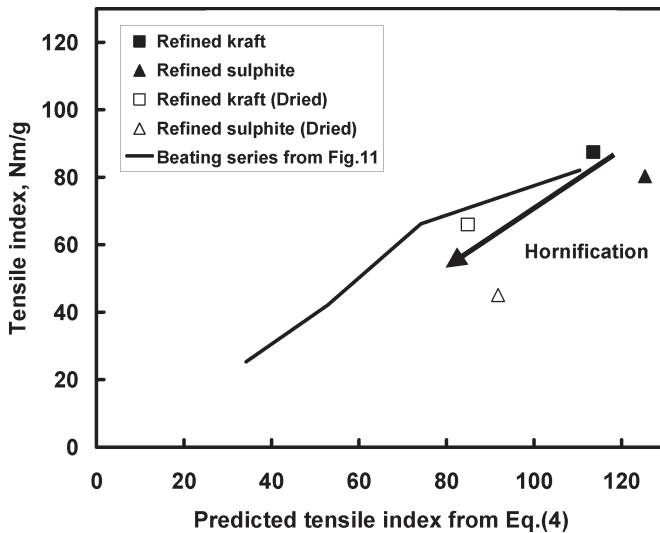
Figure 12 compares Equation (4) against measurements for bleached unrefined softwood pulps from [30] where mechanical damaging is applied to fibers. The agreement is good regardless of wood origin.

Figure 13 plots measured tensile index and Equation (4) for some dried and never dried refined kraft and sulphite pulps. The model clearly accounts for the hornification in chemical pulps. However, the model does not explain the reduction in tensile strength – due to weakening of fibers – when the cooking method is changed from kraft pulping to sulphite pulping.





**Figure 12** Equation (4) vs. measurements for unrefined bleached softwood pulps. Mechanically damaged pulps are marked with hollow symbols. The line is the same line as in Figure 11. RW=Roundwood and SC=Sawmill chips.  $w_{fiber} / t_{fiber} = 2.0$  in Equation (4).



**Figure 13** Equation (4) vs. measurements for dried and never dried kraft and sulphite pulps. The line is the same line as in Figure 11.  $w_{fiber} / t_{fiber} = 2.0$  in Equation (4).

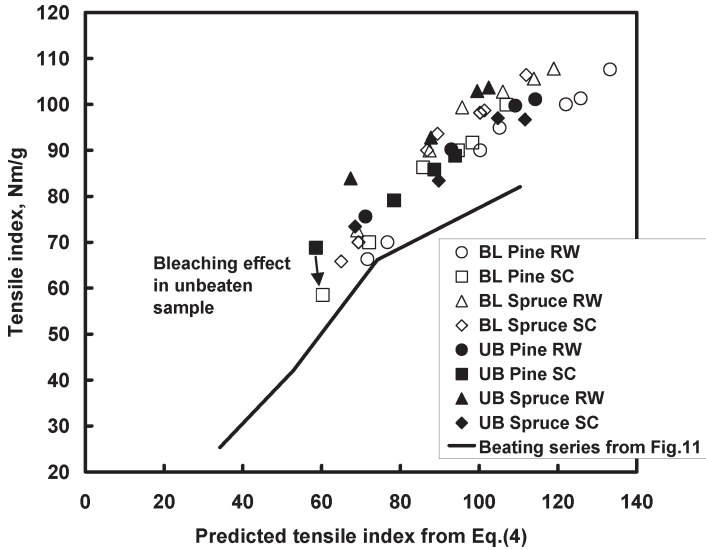


**Figure 14** Equation (4) vs. measurements using data from [33]. Refining series of bleached and unbleached spruce and pine laboratory kraft pulps from different raw materials. UB=Unbleached, BL=Bleached, RW=Roundwood and SC=Sawmill chips. The line is the same line as in Figure 11.  $w_{fiber} / l_{fiber} = 2.0$  in Equation (4).

Figure 14 compares kraft pulps made of different wood raw materials. The role of different softwood fiber dimensions seems to be insignificant. The model does not reproduce the small strength reduction caused by bleaching. Figure 15 gives the comparison for different mechanical and hardwood kraft pulp of different refining levels. The mechanical pulps fall below the line typically followed by kraft pulps.

#### 4.4 Machine made papers

All the unit processes of the paper machine affect paper properties. Figure 16 demonstrates how apparent changes with in inter-fiber bonding may actually effect little change in tensile strength. The changes seen here in the predicted tensile strength arose from changes in the Scott bond because the in-plane tensile stiffness remained constant. Probably what happened was that there was a weak layer in the sheet structure that caused changes in the Scott values even when inter-fiber bonding did not change. If such a weak layer existed, it would not influence the in-plane tensile strength.

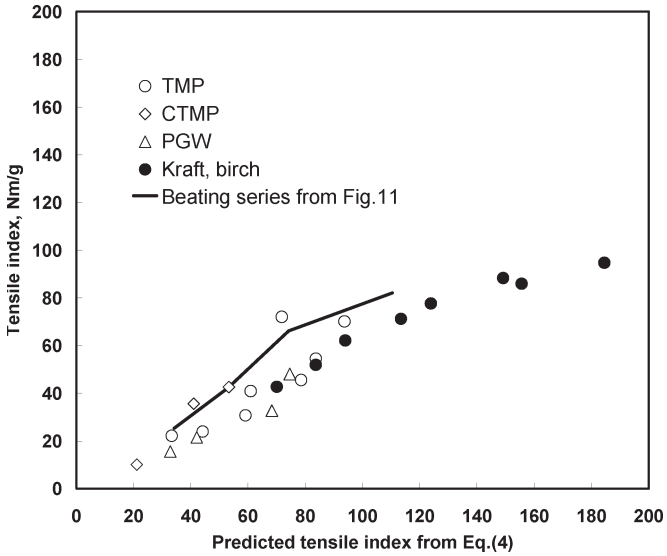


**Figure 15** Equation (4) vs. measurements for various chemical and mechanical pulp handsheets and refined to various levels. The line is the same line as in Figure 11.  $w_{fiber} / t_{fiber} = 2.0$  in Equation (4).

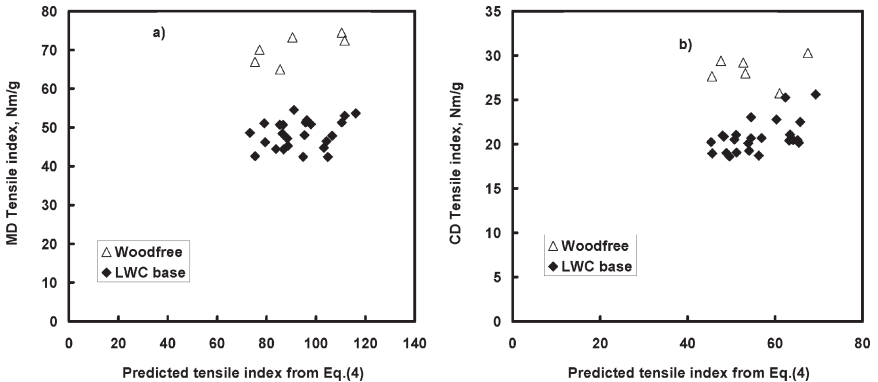


**Figure 16** Equation (4) applied to pilot paper data of GW based LWC base and woodfree furnishes.  $w_{fiber} / t_{fiber} = 2.0$  in Equation (4).

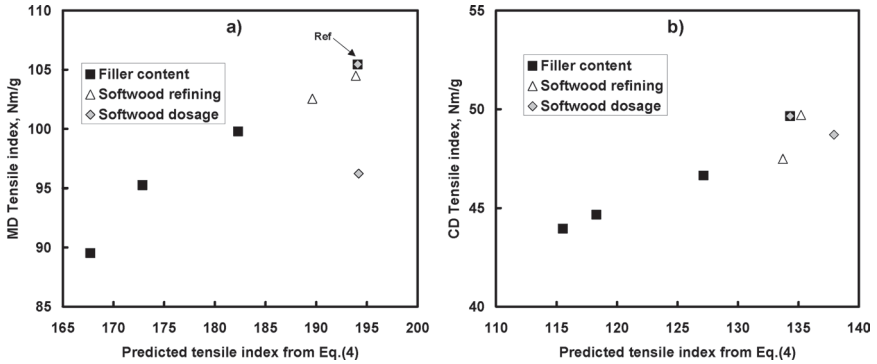


**Figure 17** Equation (4) vs. measurements for a paper machine trial [34].  $w_{fiber} / t_{fiber} = 2.0$  in Equation (4).

Figure 17 shows a fine paper example of paper machine trials where filler content, and amount and refining of softwood pulp were changed. Equation (4) captures excellently the effect of filler content and refining level, but fails to do so for the softwood pulp content.

## 5 DISCUSSION

The results presented in the previous chapter show how the macroscopic model we derived is *consistent* with a lot of different experimental data sets. Although the word *agree* was used above, we cannot really say that the model *agrees* with experiments because the strength values predicted by the model would be clearly larger than those measured if realistic fiber dimensions were used.

The situation might have been different if z-directional fracture energy values  $G_z$  had been available instead of Scott bond. Now we had to use Scott bond to calculate an estimate for  $G_z$ . The Scott bond calculation makes use of the fiber width-to-thickness ratio  $w_{fiber} / t_{fiber}$ . In order to obtain quantitative agreement with experiments, we used smaller values than the realistic values from 3 to 5. In our opinion, what this demonstrates are the problems encountered if one tries to use micromechanical approach rigorously. One simply cannot govern the complicated properties of real paper with simple geometric considerations.

In our calculation, we needed fiber width in order to calculate an estimate for the critical crack size  $a_z$  that triggers the z-dimensional fracture, Equation

(A1) in Appendix I. The fiber width  $w_f = 3.8\mu\text{m}$  that we used in our calculations yields  $a_z \approx 2\mu\text{m}$  (for sheet density  $750\text{ kg/m}^3$ ), a value that could be characteristic of the fiber surface structure. Even in the event that  $a_z$  is indeed controlled by the fiber network structure, we have reasons to believe that the theoretical estimate in Equation (A1) is an overestimate. When the same approach is used to calculate free span lengths  $l_s$  between fibers in images of sheet cross-sections, the calculated values are roughly two times larger than the values actually measured from the cross-sectional images [35]. Direct measurement of the free span length [31] would of course be more reliable than the estimate in Equation (A1).

While the fiber width-to-thickness ratio  $w_{\text{fiber}} / t_{\text{fiber}}$  that we used is unrealistically small, it does not seem to vary for a given fiber furnish. Consider softwood kraft pulp as an example. Most of the data for softwood kraft pulp fall on or close to one line when the input parameter  $w_{\text{fiber}} / t_{\text{fiber}}$  of the model is held constant. This is true for fiber orientation, wet straining, drying shrinkage and refining of many different softwood kraft pulps. The cases that deviate from the general trend include unbleached kraft pulp, mechanical pulps, some forms of fiber treatment, and starch addition.

For the starch samples of Figure 11 we happened to have nip peeling data available. This allowed the comparison of measured tensile index values with Equation (3) in Figure 18. The result confirms that the addition of starch breaks the invariance between out-of-plane and in-plane fracture energy measurements. After starch addition, proportionately more fracture energy is consumed in the out-of-plane mode than in the in-plane mode. We can only speculate how this happens. For example, it could be that delamination tests cause more fiber wall cracking and hence higher fracture energy when starch is present than when it is not. Fiber wall cracking would conceivably not be present to the same extent in the in-plane fracture.

With mechanical pulps and unbleached pulps it is plausible that the ratio  $w_{\text{fiber}} / t_{\text{fiber}}$  is so much smaller than with bleached kraft pulps that this would explain the observed difference between mechanical and chemical softwood pulps. Direct fracture energy measurements would solve the question because fiber dimensions do not appear in Equation (3). In principle the difference could also arise from bonding, in analogy to the effect of starch.

Finally, it is also possible that the high stiffness of the mechanical pulp fibers leads to lower in-plane fracture energy at the same z-directional fracture energy. According to this line of thought, the in-plane fracture of a bleached kraft sheet would consume energy in the rectification of fiber curl and “micro-compressions” at the bonding sites. Such a fracture energy mechanism would not be present with mechanical or unbleached kraft pulp fibers. In this respect it is interesting how well our model agrees with experiments for

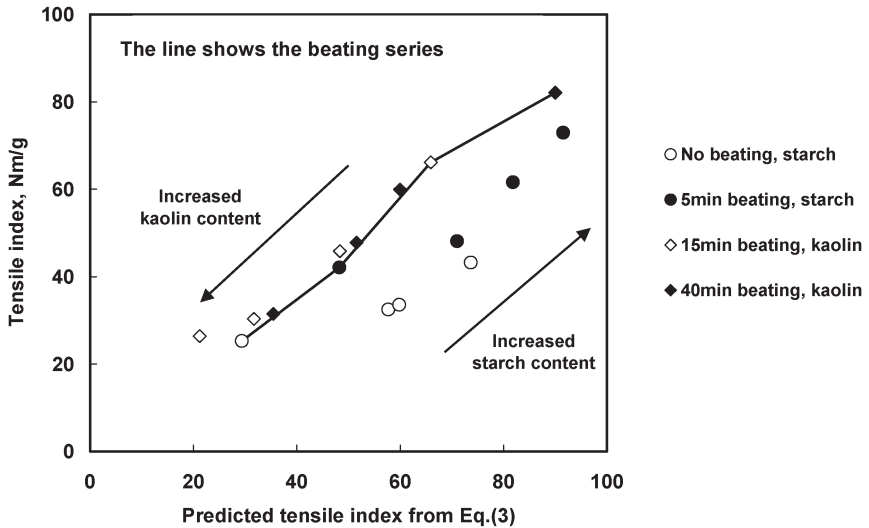


**Figure 18** Equation (3) vs. measurements for unrefined and refined softwood kraft pulps with addition of 10 to 30% kaolin and 1 to 4% starch. The samples are the same as in Figure 11. Nip peeling test was used to determine the z-directional fracture energy.

changes in refining or drying shrinkage. Both of these changes would seem to effect changes in the “activation” of fiber segments. Hence they should affect the amount of fracture energy that is consumed in the rectification of fibers. Still the invariance defined by Equation (2) holds. This suggests that the rectification of fiber curl and micro-compressions does not significantly contribute to in-plane fracture energy.

Let us then look closer at the role of fiber treatments. The model does not agree with experiments when fiber strength is altered in bleaching, Figure 14, or by different cooking methods, Figure 13. On the other hand, the model does agree with reality if fibers suffer mechanical damage. The problem lies with the invariance relationship in Equation (2). It is invalid when fibers fail the in-plane fracture mode. This becomes apparent from Figure 19 where we plot  $G/w_d$  against  $W_d/b$  for an acid vapor degradation series [36]. In that study  $b_{sheet}/b_{fiber}$  remained constant. Tensile index initially decreased dramatically and linearly as a function of zero-span strength, but Scott bond did not. The behavior here is different from another study [22] where we found that  $G/w_d$  is constant when fibers degrade.

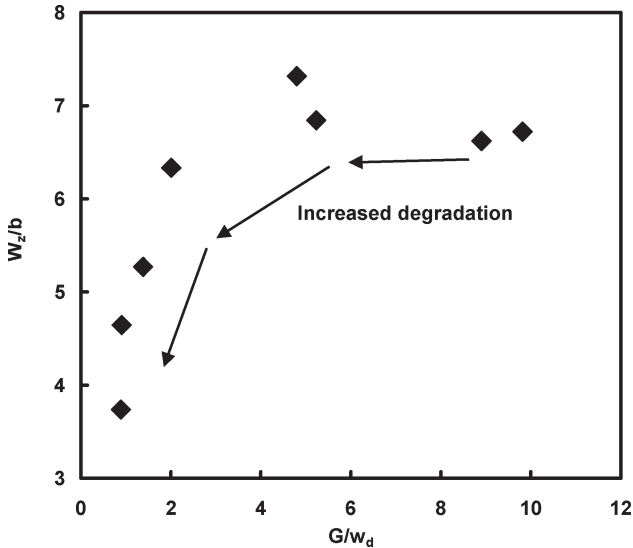


**Figure 19**  $G/w_d$  vs.  $W_z/b$  from acid vapor degradations series of softwood kraft [36].

The qualitative explanation to the effect of fiber failures is the following. When fiber strength is decreased, some fiber layers fail through fiber failure and not debonding. The z-directional fracture energy can still remain constant, as happens in Figure 19 for the initial phase of fiber degradation. However, when fibres break, the remaining number of fiber layers that debond becomes smaller than the value  $b_{sheet}/b_{fiber}$  used in Equation (2), and this leads to smaller values of tensile index than what our models predict. More detailed discussion will be presented elsewhere.

## 6 CONCLUDING REMARKS

We have presented a “macromechanical” study that connects tensile strength with the macroscopic mean values of tensile stiffness and z-directional fracture energy. The model expression agrees well with many – but not all – of the experimental datasets that we considered. The disagreements demonstrate that z-directional fracture measurements do not quite capture some aspects of inter-fiber bonding that are important for the in-plane tensile strength. Starch addition is a good example: z-directional fracture energy overestimates its effect on tensile index. The effects of low fiber strength are missing from the current analysis.

Our analysis shows why Scott bond or z-directional tensile index are not as good measures of inter-fiber bonding as is the z-directional fracture energy. In order to work back to the average z-directional fracture energy micromechanical assumptions must be made that, as we have demonstrated, are not accurate.

In spite of the current shortcomings, the approach we have presented is useful because it connects tensile strength directly to easily measurable macroscopic properties, i.e. tensile stiffness and z-directional fracture energy. These two represent the mean tensile stiffness of the fibers in paper and the mean bonding energy of inter-fiber bonds in paper. They are “effective” properties or “metafiber” properties that include the effect of the surrounding fiber network medium in which the fibers have been dried into.

## REFERENCES

1. D.H. Page. A theory for the tensile strength of paper. *Tappi* **52**(4):674–681, 1969.
2. G.G. Allan and A.N. Neogi. Fundamentals of fiber assemblages. Part III. Unifying theory for the tensile strength of paper and nonwovens. *Cellul. Chem. Technol.* **8**:297–318, 1974.
3. O. Kallmes, G. Bernier, and M. Perez. A mechanistic theory of the load-elongation properties of paper. Part 1: A uniform strain theory for paper. *Pap. Technol. Ind.* **18**(7): 222–228, 1977.
4. O. Kallmes, G. Bernier, and M. Perez. A mechanistic theory of the load-elongation properties of paper. Part 2: The characteristics of fibres taken into account. *Pap. Technol. Ind.* **18**(8):243–245, 1977.
5. O. Kallmes, G. Bernier, and M. Perez. A mechanistic theory of the load-elongation properties of paper. Part 3: The theory of the tensile failure of paper. *Pap. Technol. Ind.* **18**(9):283–285, 1977.
6. O. Kallmes, G. Bernier, and M. Perez. A mechanistic theory of the load-elongation properties of paper. Part 4: Experimental evaluation of the theory. *Pap. Technol. Ind.* **18**(10):328–331, 1977.
7. O. Kallmes, G. Bernier, and M. Perez. A mechanistic theory of the load-elongation properties of paper. A descriptive summary. *Pap. Technol. Ind.* **19**(9):311–312, 1978.
8. P. Shallhorn and A. Karnis. Tear and tensile strength of mechanical pulps. *Pulp Pap. Can.* **80**(12):TR92–TR99, 1979.
9. K. Jayaraman and M.T. Kortschot. Closed-form network models for the tensile strength of paper – a critical discussion. *Nord. Pulp Pap. Res. J.* **13**(3):233–242, 1998.
10. R.S. Seth and D.H. Page, The Stress-Strain Curve of Paper. In **The Role of Fundamental Research in Paper Making**. *Trans. 7th Fund. Res. Symp.*, (ed. J. Brander), pp 421–454, Mech. Eng. Publ., London, UK, 1983.



11. K. Niskanen and P. Kärenlampi, In-plane tensile properties. In **Paper physics**. (ed. K. Niskanen), pp 166–169, Fapet Oy, Helsinki, Finland, 1998.
12. See e.g. N.W. Ashcroft and N.D. Mermin, Solid state physics, pp 278–279, Holt Rinehart and Winston, New York, 1976; or almost any textbook on solid state physics.
13. K. Niskanen, Kraft fibers in paper – Effect of beating. In *10th International Conf. CELLUCON 98*, pp 249–260, Woodhead Publ., Cambridge, UK, 2000.
14. W.J. Batchelor and D.M.S. Wanigaratne. A new cyclic loading method for measuring sheet fracture toughness. *International Journal of Fracture* **123**(1–2):15–27, 2003.
15. O. Andersson and L. Sjöberg. Tensile studies of paper at different rates of elongation. *Svensk Pappertid.* **56**(16):615–624, 1953.
16. B.C. Donner. An heuristic model of paper rupture. In **Fundamentals of papermaking materials**, *Trans. 11th Fund. Res. Symp.*, (ed. C.F. Baker), pp1215–1247, Pira International, Surrey, UK, 1997.
17. M. Korteoja, L.I. Salminen, K.J. Niskanen and M.J. Alava. Strength distribution in paper. *Mater. Sci. Eng.* A248:173–180, 1998.
18. T. Uesaka and M. Ferahi. Principal factors controlling press room breaks. In *proc. Tappi International Paper Physics Conference*, pp229–245, San Diego, CA, USA. Tappi Press, Atlanta, USA, 1999.
19. Ø.W. Gregersen. On the assesment of effective paper web strength. Doctoral thesis, Department of Chemical Engineering, Norwegian University of Science and Technology, Trondheim, Norway, 1998.
20. J.I. Katz. Statistics and microphysics of the fracture of glass. *J. Appl. Phys.* **84**(4):1928–1931, 1998.
21. M.J. Korteoja, A. Lukkarinen, K. Kaski, D.E. Gunderson, J.L. Dahlke and K.J. Niskanen. Local strain fields in paper. *Tappi J.* **79**(4):217–223, 1996.
22. K. Niskanen, H. Kettunen and Y. Yu. Damage width: a measure of the size of fracture process zone. In **The science of papermaking**, *Trans. 12th Fund. Res. Symp.*, (ed. C.F. Baker), pp1467–1482, FRC, Lancashire, UK, 2001.
23. R. Wathén. Characterizing the Influence of Paper Structure on Web Breaks, Licentiate thesis, Department of Forest Products Technology, Laboratory of Paper Technology, HUT, Espoo, Finland, 2003.
24. A. Tanaka, H. Kettunen, K. Niskanen and K. Keitaanniemi. Comparison of energy dissipation in the out-of-plane and in-plane fracture of paper. *J. Pulp Pap. Sci.* **26**(11):385–390, 2000.
25. H. Kettunen, Y. Yu and K. Niskanen. Microscopic damage in paper. Part 2: Effect of fibre properties. *J. Pulp Pap. Sci.* **26**(7):260–265, 2000.
26. O. Schulz-Eklund, C. Fellers and G. Olofsson. Z-toughness: A new method for the determination of the delamination resistance of paper. *1987 Int'l Paper Physics Conf.*, pp 189–195. CPPA, Montreal, 1989.
27. A. Lundh and C. Fellers. The Z-toughness method for measuring the delamination resistance of paper. *Nord. Pulp Pap. Res. J.* **16**(4):298–305, 2001.
28. H. Kettunen and K. Niskanen. On the in-plane tear test. *Tappi J.* **83**(4):83, 2000.
29. A. El Maachi, S. Sapielha and A. Yelon. Angle-dependent delamination of paper.

- Part II: Determination of deformation and detachment work in paper peeling. *J. Pulp Pap. Sci.* **21**(12):J401–J407, 1995.
30. K Niskanen, H Rajatora, Statistical geometry of paper cross-sections. *J Pulp Pap. Sci.* **28**(7): 228–233, 2002.
  31. J. He, W. Batchelor and B. Johnston, A microscopic study of fibre-fibre contacts in paper. *Tappi J.* **57**(4): 292–298, 2004.
  32. G. Zhang. Effect of drying on the in-plane tensile properties of paper, Doctoral thesis, Laboratory of Paper Technology, HUT, Espoo, Finland, 2004.
  33. O. Joutsimo. Effect of mechanical treatment on softwood kraft fiber properties. Doctoral thesis, Department of Forest Products Technology, Laboratory of Pulp Technology, HUT, Espoo, Finland, 2004.
  34. M. Sundqvist. Woodfree base paper strength evaluation and management (in Finnish), Master’s thesis, Department of Forest Products Technology, HUT, Espoo, Finland, 2003.
  35. K. Niemi, T. Hjelt, J. Asikainen, K. Niskanen, unpublished report of KCL, 2001.
  36. R. Wathén, O. Joutsimo and T. Tamminen. In **Advances in Paper Science and Technology**, *Trans. 13th Fund. Res. Symp.*

## APPENDIX I

We employ linear elastic fracture mechanics also in z-direction. We set the geometry factor  $\beta = 1$  for simplicity. Pores are the “defects” that trigger delamination. The typical dimension of such a pore is proportional to the in-plane free span length between two adjacent fibers, and therefore the critical crack size  $a_z$  is

$$a_z = \frac{l_s}{2} = \frac{1}{2} \cdot w_{\text{fiber}} \cdot \frac{\phi}{1 - \phi} = \frac{1}{2} \cdot w_{\text{fiber}} \cdot \left( \frac{\rho_{\text{fiber}}}{\rho_{\text{sheet}}} - 1 \right), \quad (\text{A1})$$

where  $\phi$  is sheet porosity,  $w_{\text{fiber}}$  is fiber width, and  $\rho_{\text{fiber}}$  and  $\rho_{\text{sheet}}$  are the densities of fibers and sheet, respectively. Equation (A1) is motivated geometrically in Figure A1. This simple view ignores the effect of fiber orientations in-plane and out-of-plane.

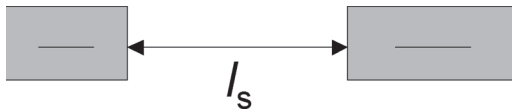


**Figure A1** Geometric derivation of Equation (A1). Porosity is then given by,

$$\phi = \frac{l_s}{l_s - w_{\text{fiber}}}, \text{ from which Equation (A1) follows.}$$

Since pores carry no stress, the z-directional elastic modulus  $E_z$  is, to first approximation, proportional to  $1 - \phi$ , or

$$E_z = E_{fiber} \cdot \frac{\rho_{sheet}}{\rho_{fiber}}, \quad (A2)$$

where  $E_{fiber}$  is a parameter describing the transverse stiffness of fibers. This approximation ignores all inhomogeneities in the local stress states.

We first calculate the z-directional tensile strength  $T_z$  from z-directional fracture energy  $G_z$ :

$$T_z = \sqrt{\frac{G_z \cdot E_z}{\pi \cdot a_z}}. \quad (A3)$$

The inversion of this expression allows us to estimate z-directional fracture energy if z-directional tensile strength is given:

$$G_z = \frac{\pi \cdot T_z^2}{E_{fiber}} \cdot \frac{\rho_{fiber}}{\rho_{sheet}} \cdot \frac{w_{fiber}}{2} \cdot \left( \frac{\rho_{fiber}}{\rho_{sheet}} - 1 \right) \quad (A4)$$

Scott bond  $W_z$  measures tensile energy absorption in z-direction, or

$$W_z = \frac{1}{2} \cdot \frac{T_z^2 \cdot t_{sheet}}{E_z} = \frac{1}{\pi} \cdot \frac{G_z \cdot t_{sheet}}{w_{fiber} \cdot \left( \frac{\rho_{fiber}}{\rho_{sheet}} - 1 \right)} \quad (A5)$$

where  $t_{sheet}$  is sheet thickness. This is a small strain approximation that gives a lower bound for  $W_z$ . Rearranging Equation (A5) leads to

$$G_z = \pi \cdot W_z \cdot \frac{w_{fiber}}{t_{sheet}} \cdot \left( \frac{\rho_{fiber}}{\rho_{sheet}} - 1 \right). \quad (A6)$$

## Transcription of Discussion

# TENSILE STRENGTH OF PAPER REVISITED

*Kaarlo Niskanen, Jari Sirviö and Rolf Wathén*

KCL Science and Consulting, P.O.Box 70, FIN – 02151 ESPOO, FINLAND

*Derek Page*

I am glad you made that comment about fibre strength and fibre breakage because I was going to raise it. I do not know whether it is well known or not, but if you break a piece of paper in tensile, fibres break, but no fibres break outside the region of rupture. This means that, if that is absolutely true, when the first fibre fails, that is what triggers sheet rupture. This necessarily follows from those two experimental findings. In the last 40 years, I have suggested several times that maybe somebody should look at that a little more closely and nobody has, of course.

*Kaarlo Niskanen*

No comment.

*Joel Pawlak*      North Carolina State University

I was wondering if you could comment on how your model would interpret the effect of drying restraint on tensile strength.

*Kaarlo Niskanen*

That comes basically through tensile stiffness. We do, of course, also expect that if you let the sheet shrink freely, then the inter-fibre bonding is probably going to be bigger than if you have a large drying strain. I think that actually Fellers and Wahlström demonstrated that but in my opinion, the biggest effect comes through tensile stiffness. That is actually one of the reasons we ended up working in this line: because tensile stiffness and strength often have a strong correlation.

## *Discussion*

*James Watkins*      Procter and Gamble

I have a comment and then there will be a question, I promise. Definitely coming out on the side of fibre chemistry. It is easy once you have a sheet with properties to measure that then we can make models so I always think that there is going to be room for the fibre bonding. But my question is that you implied a defect size. Is there evidence on the defect size, which you suggested was on the scale of fibre, to say get back to what Dr. Page mentioned?

*Kaarlo Niskanen*

If I understand correctly what you are asking, then you can of course work back from tensile strength using fracture mechanics and calculate what the value of the defect size should be. That is, for example, what I believe Benjamin did to get those values. The other thing is that I showed you the map of debonded areas where you see areas where bonds fail and from that map you could measure the size of the defects. You can see where the sheet is going to fail often well before it actually fails due to the accumulation of debonding.

*James Watkins*

That's on the scale of the size of the fibre?

*Kaarlo Niskanen*

Yes, fibre length scale, similar size.

*Tetsu Uesaka*      Mid Sweden University

This is not a question, just a comment. You mentioned in your summary slide that the microscopic details may not be so important, and I think I would agree with this on the basis of the recent progress in the stochastic fracture mechanics of disordered materials. They all show that, with all these remarkably different microscopic structures, as well as different microscopic properties, all the fracturing processes are remarkably similar. As well, all these averaging procedures actually predict this so-called defect size, which is in fact not an ordinary defect, but actually a bunch of defects clustered together, which appear just before the failure. This really fits with most of the typical defect sizes which appear in fracture mechanics formulations. So, in that sense, things are converging into one story there, but still we have not really

connected together the physics behind tensile strength that we are talking about. So, my last comment from the practical viewpoint, is it the kind of problem we should solve or not?

*Kaarlo Niskanen*

In a lot of the work we do on paper properties, the problem is that the measurements we do are somehow imperfect. There are lots of artifacts that may contribute to the measurements themselves.

*Gary Baum*      PaperFuture Technologies LLC

Nice presentation, Kaarlo. I have a question about defect size. Someone once told me that paper was nothing but a collection of defects.

*Kaarlo Niskanen*

Correct.

*Gary Baum*

I thought that that person was our Chairman today, but I asked him about it once and he said “No, no, no!”. Thinking about the pictures that we saw with the opening presentation yesterday, it certainly does look like a collection of defects. Could you comment on that?

*Kaarlo Niskanen*

Not terribly well, but I do think that one of the key benefits or strengths of paper, not in a mechanical sense but in a more general sense, is the fact that the structure is completely disordered, that you have all kinds of pores between fibres that are like local defects. If we had a solid block with a very ordered structure, we would also have a very, very brittle structure. This collection of defects triggers local debonding here and there, and so it will help very much to distribute the external load around the whole sheet.

*Lars Wågberg*      KTH

I think the influence of additives is an important point and I can very much appreciate your arguments regarding it, that is if you are studying a paper from a well-beaten fibre where the full potential of the fibres has been utilised.

## *Discussion*

What we are trying to convince people about, Tom Lindström and myself, is that beating should be avoided and replaced by chemical tailoring via, for example, Bipolar Activators or Polyelectrolyte Multilayering. This would allow us both to utilise the inherent properties of the fibres and to avoid the negative effects of beating.

## *Kaarlo Niskanen*

Definitely yes. You know, physics basically explains what is going on, but it does not solve the problems of how to make better paper. That is where you guys come in.